Copyright © 2013 Tech Science Press CMES, vol.90, no.6, pp.439-462, 2013

A Line Model-Based Fast Boundary Element Method for the Cathodic Protection Analysis of Pipelines in Layered Soils

L.Q. Liu[1], **H.T. Wang**[1,2]

Abstract: A line model-based fast boundary element method (BEM) is presented for the large-scale cathodic protection (CP) analysis of three-dimensional pipelines in layered soils. In this approach, pipelines are treated as lines with potentials assumed constant over the cross-section and the boundary integrals happen on the associated cylindrical surfaces. The advantage of this model is that pipelines can be meshed with line elements while the boundary integrals are based on the original shapes. Therefore, the number of unknowns is significantly reduced with accuracy effectively retained. A unified formulation of the multipole moments is developed for the mixed boundary element types in the framework of the fast multipole method in order that large-scale BEM problems by using the line model can be solved on a common desktop computer. An interface boundary integral equation is employed to treat the multi-layered soils with a single-domain formulation. Numerical results demonstrate validity of the proposed method and its potential for large-scale CP analysis of pipelines in multi-domains.

Keywords: Boundary element, line model, fast multipole, cathodic protection, pipeline, layered soil.

1 Introduction

Corrosion is one of the most severe problems affecting safety of structures in modern industries. To prevent structural failures due to corrosion, the cathodic protection (CP) technique based on galvanic action or impressed current has been widely applied. In order to design a CP system, knowledge of distributions of the current density and the electrochemical potential is required. To achieve this much effort has been made using various empirical formulae or numerical methods. As a

[1] Institute of Nuclear & New Energy Technology, Tsinghua University, Beijing, 100084, P. R. China
[2] Corresponding author. Tel.: + 86 10 6279 7882; fax: + 86 10 6279 7136. Email address: wanght@tsinghua.edu.cn (H. Wang)

boundary-type numerical method, the boundary element method (BEM) is particularly suitable for modeling a CP system since only the surfaces or interfaces need to be meshed. This feature significantly reduces the modeling complexity compared with other volume-meshing numerical methods. Applications of the BEM for the CP analyses have been continuously reported (Druesne, Paumelle and Villon 2000, Miltiadou and Wrobel 2002 and 2003, Wrobel and Miltiadou 2004, Ridha, Amaya and Aoki 2005, De Lacerda and Da Silva 2006, Kyung, Tae and Lee 2007, Metwally, Al-Mandhari, Gastli and Al-Bimani 2008, Butler, Kassab, Chopra and Chaitanya 2010).

Conventionally, the coefficient matrix arising from the BEM is dense with memory requirement of $O\left(N^2\right)$, where N is the number of unknowns. To solve this equation system with direct or iterative algorithms $O\left(N^2\right) \sim O\left(N^3\right)$ operations are needed. This feature becomes a bottleneck in efficiency to the standard BEM. In order to achieve large-scale BEM solutions, several fast algorithms have been implemented in this field. Particularly, the fast multipole method (FMM) proposed by Rokhlin and Greengard (1985 and 1997) is one of the most reported approach with both storage and operations reduced to $O(N)$. Formulae and applications of the fast multipole BEM have been well documented (Yoshida 2001, Nishimura 2002, Chen and Chen 2004, Liu, Nishimura and Otani 2005, Liu, Nishimura, Otani and colleagues 2005, Chen, Chen, Kao and Lee 2009, Dondero, Cisilino and Pablo 2011, Wang and Yao 2011). For the large-scale CP analysis using the fast multipole BEM, one can refer to the work of Aoki and his colleagues (Amaya and Aoki 2003, Aoki, Amaya, Urago and Nakayama 2004).

In the CP systems of the oil & chemical industries, underground pipelines are commonly encountered structures. Compared with typical pipe diameters (denoted by a) in the meter scale, lengths of the pipelines (denoted by l) usually extend in kilometers. To model such structures using standard boundary elements, an extremely large number of elements will be generated. A natural method to handle this difficulty is to simplify the pipelines to lines in shape by assuming $a \ll l$ (Adey and Niku 1992, Amaya and Aoki 2003). Therefore, line elements can be used and the number of unknowns is effectively reduced. However, certain loss of accuracy might be expected due to this artificially introduced shape degeneration and the resulting absence of the double layer integral in the standard boundary integral equation (BIE). Another approach is to use Fourier elements in which the current density and potential are approximated by complex Fourier expansion series (Amaya and Aoki 2003, Aoki, Arnaya and Imamori 2008). Using this method, the original shape of the pipelines is retained and circumferential variance of the corrosion field can be identified. In addition, line elements can be used so that the number of elements is effectively reduced. The only issue seems to be that the number of unknowns is not reduced compared with standard boundary elements. As a tradeoff between these two approximation methods, one can notice that the current density and potential remain approximately constant over the cross-sectional area of the pipes compared with their distributions along the pipe axial direction. This feature may be used for the only simplification of the pipe modeling with number of unknowns reduced and accuracy reasonably retained at the same time.

In this paper, a line model-based fast BEM is presented for the large-scale CP analyses of three-dimensional pipelines in layered soils. This line model assumes the current density and potential remain constant at any cross-section of the pipes and vary only on the length direction. Therefore, pipelines can be meshed with line elements. Compared with standard meshing, this simplification can increase the pipeline scales to be analyzed at least one order of magnitude higher. For each line element, the boundary integrals happen on the original cylindrical shape of the corresponding pipe and can be evaluated analytically or by one-dimensional Gaussian quadrature. This feature assures reasonable accuracy of the line model by preventing shape degeneration. The BEM is accelerated by the FMM in order that large-scale CP analyses are performed on a personal desktop computer. In order to combine multiple boundary element types into the framework of the FMM, a unified formulation of the multipole moments is established. The advantage is that the rest expansion and translation formulations of the FMM remain unchanged, leading to a minimum modification of any in-hand standard FMM code. In order to effectively treat layered soils, an interface integral BEM initially proposed by Gao and Wang (2009) is employed herein to govern this multi-domain problem with a single-domain formulation. In the numerical examples, validity and large-scale capacity of the proposed method for the CP analysis of pipelines embedded in multi-domains are demonstrated.

2 Line model-based BEM for pipelines in layered soils

In this section, the interface integral BEM for layered soils embedded with pipelines is briefly reviewed, followed by a line boundary element model presented for modeling pipelines in the CP analyses. Thirdly, basic expansion formulae of the fast multipole BEM governing the CP problem are summarized, highlighting a unified formulation of the multipole moments developed for integrating both standard and line boundary elements.

2.1 Interface integral BEM for layered soils embedded with pipelines

The CP system in a three-dimensional homogenous domain is governed by the Laplace equation. The associated boundary integral equation (BIE) is expressed as,

$$c(x)\phi(x)+\int_S \frac{\partial \Phi^*(x,y)}{\partial n}\phi(y)\,dS(y)=\int_S \Phi^*(x,y)\left[-\frac{1}{k}I(y)\right]dS(y) \tag{1}$$

where x and y denote the source and field points at the boundary S, respectively; ϕ and I are the boundary potential and current density respectively; n is the outward normal to the boundary S; k is the conductivity; $c(x)$ is 0.5 for smooth boundaries; $\Phi^*(x,y)$is the kernel function for the three-dimensional CP problem defined as,

$$\Phi^*(x,y)=\frac{1}{4\pi r} \tag{2}$$

with r being the distance between x and y. For the multi-domain CP systems such as layered soils embedded with pipelines, an interface integral BEM initially proposed by Gao and Wang (2009) is applied for governing this problem with a single-domain BIE formulation given by,

$$\begin{aligned}&\hat{k}(x)\phi(x)+\sum_i \int_{S_i^0+S_i^p} k_i\frac{\partial \Phi^*(x,y)}{\partial n}\phi(y)\,dS(y)+\sum_{i,j}^{i\neq j}\int_{S_{ij}^0}\Delta k\frac{\partial \Phi^*(x,y)}{\partial n'}\phi(y)\,dS(y)\\&=-\sum_i\int_{S_i^0+S_i^p}\Phi^*(x,y)I(y)\,dS(y)\end{aligned} \tag{3}$$

where $S_i^0$is the independent boundary of the i-th soil layer denoted by V_i, $S_i^p$the boundary of pipelines in V_i, $S_{ij}^0$the interface of the i-th and j-th soil layers, k_i the conductivity of the i-th soil layer, n' the normal direction to S_{ij}^0pointing from the i-th to the j-th soil layer. $\hat{k}(x)$and $\Delta k$are given by (Gao and Wang 2009),

$$\hat{k}(x)=\begin{cases}\frac{k_i}{2}, & x\in S_i^0+S_i^p\\ \frac{k_i+k_j}{2}, & x\in S_{ij}^0\\ k_i, & x\in V_i\\ 0, & x\notin (V\cup S)\end{cases} \tag{4}$$

$$\Delta k=k_i-k_j \tag{5}$$

provided x is on the smooth boundaries. By defining new variables $\hat{\phi}$and $\hat{I}$as,

$$\begin{aligned}&\hat{\phi}(x)=\begin{cases}k_i\phi(x), \; x\in S_i^0+S_i^p\\ (k_i-k_j)\phi(x), \; x\in S_{ij}^0\end{cases}\\&\hat{I}(x)=\begin{cases}-I(x), \; x\in S_i^0+S_i^p\\ 0, \; x\in S_{ij}^0\end{cases}\end{aligned} \tag{6}$$

Eq. (3) is rewritten as,

$$\begin{aligned} &\hat{c}(x)\,\hat{\phi}(x) + \int_{\sum S_i^0 + S_i^p + S_{ij}^0} \frac{\partial \Phi^*(x,y)}{\partial n}\hat{\phi}(y)\,dS(y) \\ &= \int_{\sum S_i^0 + S_i^p + S_{ij}^0} \Phi^*(x,y)\,\hat{I}(y)\,dS(y) \end{aligned} \tag{7}$$

where $\hat{c}(x)$is defined as,

$$\hat{c}(x) = \begin{cases} \frac{1}{2},\ x \in S_i^0 + S_i^p \\ \frac{1}{2}\frac{k_i + k_j}{k_i - k_j},\ x \in S_{ij}^0 \\ 0,\ x \notin (V \cup S) \end{cases} \tag{8}$$

The convenience of Eq. (7) is that a BIE equivalent to the standard single-domain formulation is established. Therefore, any in-hand BEM solver available for the single-domain Laplace equation can be applied directly to solve Eq. (7). When $\hat{\phi}$and $\hat{I}$are obtained, ϕ and I are readily derived with Eq. (6).

2.2 Line model

In order to discretize Eq. (7) we use collocation method and piece-wise constant boundary element. For the pipelines, meshing with standard boundary elements such as triangular or quadrilateral shapes typically generates a large number of unknowns, thus having a significant limitation on the pipeline scales to be analyzed. Consider the fact that current density and potential over the cross-section of a pipe is approximately constant compared with its distribution along the length direction of the pipe, it is reasonable to assume the corrosion field at the pipeline surfaces varies only on the length direction and remains constant circumferentially. Therefore, pipelines can be meshed with line elements, leading to the associated number of unknowns significantly reduced. In addition, for each line element, the boundary integrals in Eq. (7) happen on the origin shape of the corresponding pipe sector in order to prevent loss of accuracy due to any shape degeneration.

Since the current density and potential have been assumed independent of their circumferential locations on the pipe, the associated boundary integrals can be evaluated analytically or by one-dimensional Gaussian quadrature. Consider a constant line element with its cylindrical boundary denoted by $S_i^{p,E}$ as shown in Fig. 1, the boundary integrals can be deduced as,

$$\int_{S_i^{p,E}} \Phi^*(x,y)\hat{I}(y)\,dS(y) = \frac{a_i \hat{I}_i^E}{4\pi}\int_0^{2\pi} \ln \frac{R_2(\theta)+\frac{L_i}{2}-z_x}{R_1(\theta)-\frac{L_i}{2}-z_x}\,d\theta \tag{9}$$

$$\begin{aligned}&\int_{S_i^{p,E}} \frac{\partial \Phi^*(x,y)}{\partial n}\hat{\phi}(y)\,dS(y)\\ &= \frac{a_i\hat{\phi}_i^E}{4\pi}\int_0^{2\pi} \frac{a_i-\rho_x\sin\theta}{\rho_x^2-2\rho_x a_i\sin\theta+a_i^2}\left[\frac{\frac{L_i}{2}+z_x}{R_1(\theta)}+\frac{\frac{L_i}{2}-z_x}{R_2(\theta)}\right]d\theta\end{aligned} \tag{10}$$

where $\hat{\phi}_i^E$ and $\hat{I}_i^E$ are values of $\hat{\phi}$and $\hat{I}$ at this element; a_i and L_i are the cross-sectional radius and length of the element, respectively; $\rho_x$and $z_x$are the radial and azimuth coordinates of x respectively under the local Cylindrical coordinate system (ρ,θ,z)(see Fig. 1) originated at the center of the element; $R_1(\theta)$and $R_2(\theta)$ as shown in Fig. 1 represent distances between x and y when y moves on the circular lines at the two ends of the element. Eqs. (9) and (10) can be evaluated by the one-dimensional Gaussian quadrature effectively.

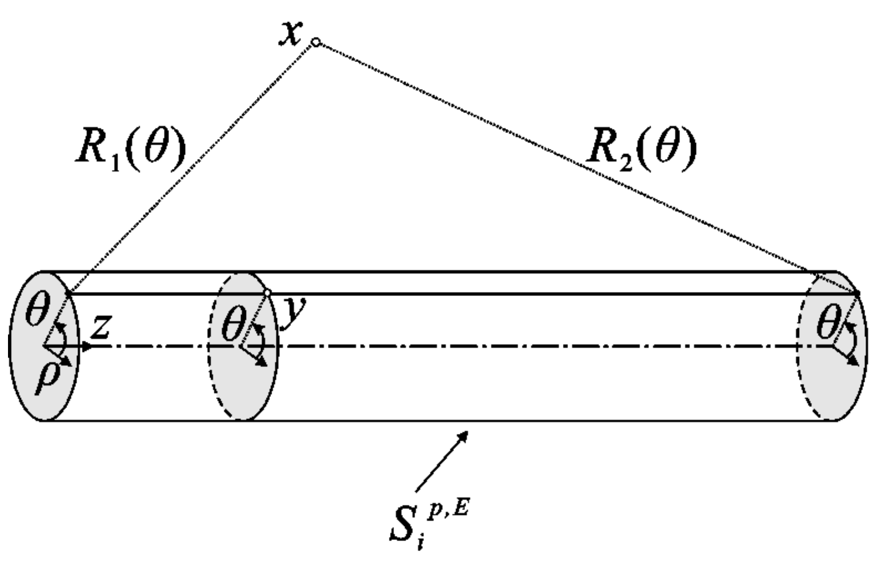

Figure 1: Integration scheme of the line element

In the case of $\rho_x = 0$, which indicates x is on the extension line of the element, an analytical result can be derived,

$$\int_{S_i^{p,E}} \Phi^*(x,y)\,\hat{I}(y)\,dS(y) = \frac{a_i \hat{I}_i^E}{2} \ln\left(\frac{R_2 + \frac{L_i}{2} - z_x}{R_1 - \frac{L_i}{2} - z_x}\right) \tag{11}$$

$$\int_{S_i^{p,E}} \frac{\partial \Phi^*(x,y)}{\partial n} \hat{\phi}(y)\,dS(y) = \frac{\hat{\phi}_i^E}{2}\left(\frac{\frac{L_i}{2} + z_x}{R_1} + \frac{\frac{L_i}{2} - z_x}{R_2}\right) \tag{12}$$

Specifically, when x and y belong to the same element, a further simplification of the analytical result can be derived provided x is collocated at the center of the element,

$$\int_{S_i^{p,E}} \Phi^*(x,y)\,\hat{I}(y)\,dS(y) = \frac{a_i \hat{I}_i^E}{2} \ln\left(\frac{\sqrt{4a_i^2 + L_i^2} + L_i}{\sqrt{4a_i^2 + L_i^2} - L_i}\right) \tag{13}$$

$$\int_{S_i^{p,E}} \frac{\partial \Phi^*(x,y)}{\partial n} \hat{\phi}(y)\,dS(y) = \frac{\hat{\phi}_i^E L_i}{\sqrt{4a_i^2 + L_i^2}} \tag{14}$$

2.3 Fast multipole BEM with mixed boundary elements

Formulae and applications of the fast multipole BEM have been well documented. The basic idea of the fast multipole BEM is to establish appropriate multipole and local expansion series of the kernel functions governing the corresponding physical equation. In this section, a unified formulation of the multipole moments is established for treating mixed boundary element types, and the follow-up expansion and translation formulae of the fast multipole BEM for the Laplace equation governing CP problems are summarized.

Consider a reference point O close to y and a threshold of $\left|\overrightarrow{Oy}\right| < \left|\overrightarrow{Ox}\right|$ is satisfied, the boundary integrals in Eq. (7) can be expanded around O to the following compact series according to the literature (Yoshida 2001),

$$\begin{aligned} &\int_S \Phi^*(x,y)\,\hat{I}(y)\,dS(y) = \tfrac{1}{4\pi} \sum_{n=0}^{\infty} \sum_{m=-n}^{n} \overline{S_{nm}}\left(\overrightarrow{Ox}\right) c_{nm}^{\phi}(O) \\ &\int_S \tfrac{\partial \Phi^*(x,y)}{\partial n} \hat{\phi}(y)\,dS(y) = \tfrac{1}{4\pi} \sum_{n=0}^{\infty} \sum_{m=-n}^{n} \overline{S_{nm}}\left(\overrightarrow{Ox}\right) c_{nm}^{I}(O) \end{aligned} \tag{15}$$

where

$$
\begin{aligned}
c_{nm}^{\phi}(O) &= \int_S R_{nm}\left(\overrightarrow{Oy}\right)\hat{I}(y)\,dS(y) \\
c_{nm}^{I}(O) &= \int_S \frac{\partial R_{nm}\left(\overrightarrow{Oy}\right)}{\partial n}\hat{\phi}(y)\,dS(y)
\end{aligned}
\tag{16}
$$

Herein S_{nm} and R_{nm} are called solid spherical harmonic functions as defined in the literature (Yoshida 2001), c_{nm}^{ϕ} and c_{nm}^{I} are called the multipole moments. The essence of Eq. (15) is that the multipole moments are independent of x. Hence they are calculated once and can be repeatedly used for many source points to evaluate the boundary integrals.

One can notice that Eq. (16) is independent of the element type. Therefore, in the case of existences of both surface and line elements, their contributions to the multipole moments can be evaluated by choosing different strategies and then accumulated directly in a unified formulation. We take c_{nm}^{ϕ} as an example,

$$
c_{nm}^{\phi}(O) = \sum \hat{I}_i^E \int_{S_i^0+S_{ij}^0} R_{nm}\left(\overrightarrow{Oy}\right)dS + \sum a_i \hat{I}_i^E \int_{-\frac{L_i}{2}}^{\frac{L_i}{2}} \int_0^{2\pi} R_{nm}\left(\overrightarrow{Oy(l,\theta)}\right)d\theta dl \tag{17}
$$

where the former part is based on the standard surface element integration; the latter part is based on the line element integration, which can be evaluated by using standard two-dimensional Gaussian quadrature.

Consider another reference point O' close to x and a threshold of $\left|\overrightarrow{O'x}\right| < \left|\overrightarrow{O'y}\right|$ is satisfied, the boundary integrals can be expanded around O' as a 'local expansion' form (Yoshida 2001),

$$
\begin{aligned}
\int_S \Phi^*(x,y)\hat{I}(y)\,dS(y) &= \frac{1}{4\pi}\sum_{n=0}^{\infty}\sum_{m=-n}^{n} R_{nm}\left(\overrightarrow{O'x}\right)d_{nm}^{\phi}(O') \\
\int_S \frac{\partial\Phi^*(x,y)}{\partial n}\hat{\phi}(y)\,dS(y) &= \frac{1}{4\pi}\sum_{n=0}^{\infty}\sum_{m=-n}^{n} R_{nm}\left(\overrightarrow{O'x}\right)d_{nm}^{I}(O')
\end{aligned}
\tag{18}
$$

where d_{nm}^{ϕ} and d_{nm}^{I} are called the local moments. They can be derived by a linear mapping operator on the multipole moments instead of be evaluated directly (Yoshida 2001),

$$
d_{nm}(O') = \sum_{n'=0}^{\infty}\sum_{m'=-n'}^{n'} (-1)^n \overline{S_{n+n',m+m'}}\left(\overrightarrow{OO'}\right)c_{n'm'}(O) \tag{19}
$$

Herein we omit the upper index of the multipole and local moments since the corresponding expansions of the two boundary integrals are unified.

In the framework of the fast multipole BEM, an adaptive octal tree will be generated in terms of locations of the boundary elements. By performing recursive operations on this tree, an upward stage followed by a downward stage is established in order to calculate and store the multipole and local moments respectively. An entire operation of the tree, which costs only $O(N)$ in both computational time and memory, represents one operation of the coefficient matrix-vector multiplication at each iterative step of the GMRES without explicit storage of the matrix. Therefore, the fast multipole BEM is $O(N)$ provided the equation system is well preconditioned.

3 Numerical results

A C++-based BEM code has been developed for the three-dimensional CP analysis of the layered soils embedded with pipelines based on the presented method. In the code, each entry is calculated and stored as an *eight-byte* value. Two solvers are employed in the code, namely 1) the conventional preconditioned GMRES and 2) the fast multipole BEM. In order to assess the validity and large-scale efficiency of the presented method, a number of numerical tests have been carried out, highlighting the modeling of pipelines, multi-layered soils and the associated large-scale calculations. The code runs on a desktop computer with a processor of AMD 2800+ and physical memory of 2GB.

In the following, the relative error of convergence in GMRES is taken to be 10^{-5}; the truncated number of multipole and local expansions of the fast multipole BEM is taken to be 10; the Newton-Raphson (N-R) method is used to treat the nonlinear boundary conditions due to the polarization curve.

3.1 Potentials or current densities along the pipelines in a single domain: a comparison

This test involves the CP analysis of a $30 \times 10 \times 10$ homogenous domain containing 2 straight pipelines along its long-axial central line as shown in Fig. 2. Each pipeline is 12.0 in length and 0.4 in diameter. The conductivity of the domain is taken to be $k = 5.0$. The left and right ends of the domain are subjected to given potentials as $\bar{\phi} = 150$ and $\bar{\phi} = 10$ respectively, and the rest of its boundaries are insulated. Three cases of the boundary conditions applied to the pipelines as listed in Table. 1 are studied, namely the given potential, current density and nonlinear potential-current density $(\phi - I)$ curve as shown in Fig. 3. Herein the nonlinear curve is used only for the purpose of testing the accuracy of the N-R method. In each case, the conventional model meshed with triangular elements and the line model are employed respectively for comparison. The meshing makes sure the two element types have the same mesh size along the length direction of the pipelines. The associated numbers of unknowns are listed in Table. 1. GMRES is adopted as the BEM solver. The numerical results are also compared with the finite element method (FEM) by using the commercial software ABAQUS.

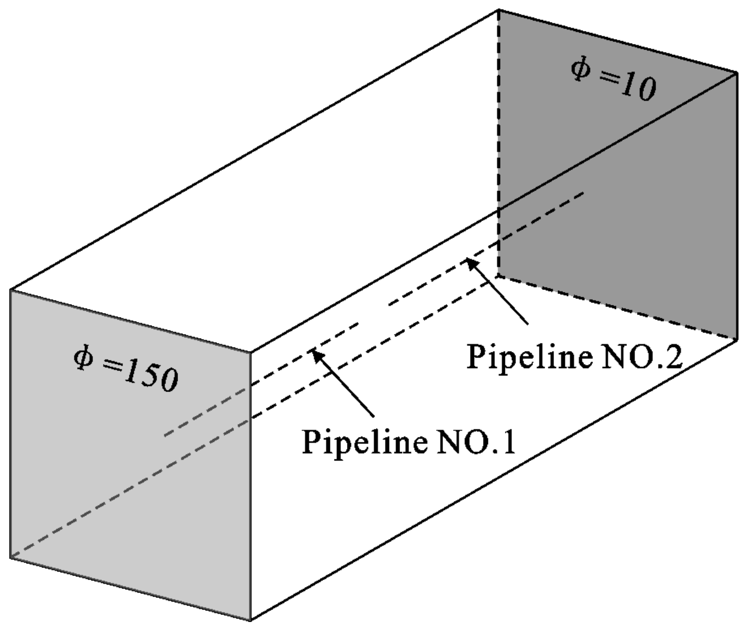

Figure 2: Scheme of a homogenous domain containing pipelines

Table 1: Boundary conditions of the pipelines and the number of unknowns

Case No.		1	2	3
Given boundary condition		Potential $\bar{\phi} = 80$	current density $\bar{I} = 100$	$\phi - I$ relation see Fig. 3
Number of unknowns per pipeline	Conventional	738		
	Line model	20		
Total number of unkowns	Conventional	12,676		
	Line model	11,240		

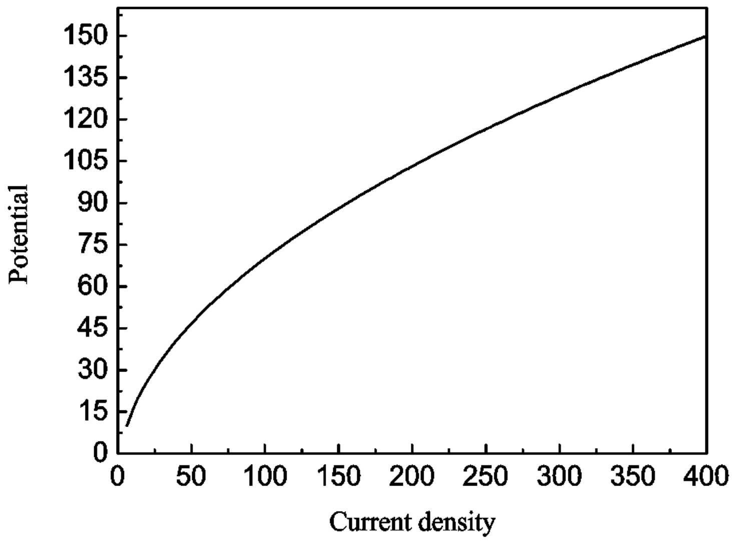

Figure 3: Nonlinear $\phi - I$ relations

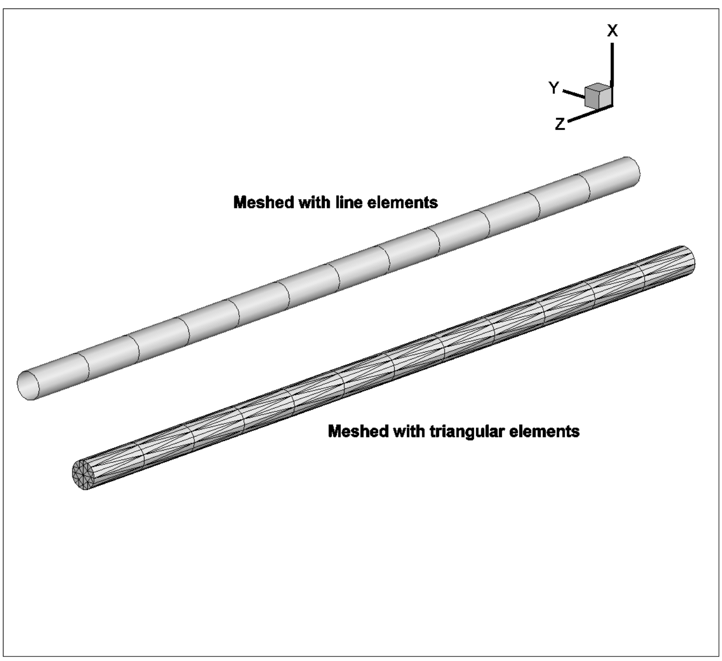

Figure 4: A comparison of the pipeline meshed with triangular and line elements

Fig. 4 show a comparison of the pipeline meshed with triangular and line elements. In Fig. 5, the results of current densities along each pipeline by using the two BEM models and the FEM in Case No. 1 are compared. In Figs. 6 and 7, the results of potentials along each pipeline in Cases No. 2 and 3 are compared, respectively. For the conventional BEM model and the FEM model, the values come from the line of $\theta = 0$ (see Fig. 1) at the cylindrical surface of each pipeline.

It is shown that the results of the line model in all the three cases of boundary conditions agree well with those of the conventional BEM and FEM models, demonstrating validity and high accuracy of the proposed method in modeling pipelines in the CP analysis. The only small discrepancy is observed at the ends of the pipelines, which is due to the local geometrically discontinuity at these locations that cannot be identified by the line model. According to Table.1, the number of unknowns per pipeline by using the line model is one order of magnitude much less than the conventional model. Therefore, modeling large-scale pipelines becomes possible by using the line model.

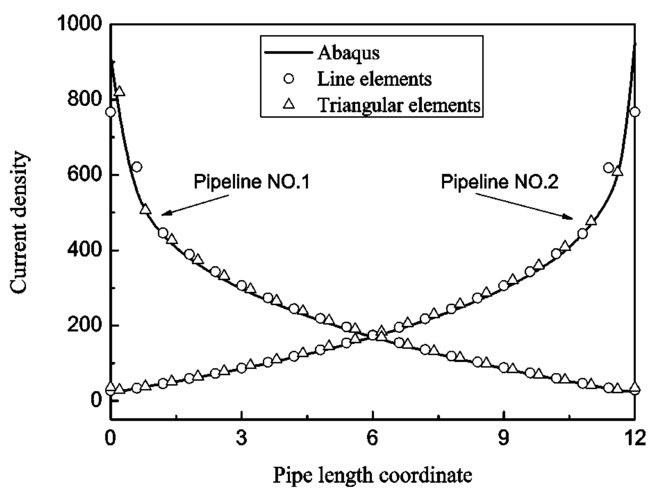

Figure 5: Current densities along the two pipelines in Case No. 1

3.2 *Potentials or current densities along the pipelines in layered domains: a comparison*

This test involves the CP analysis of a $15 \times 5 \times 10$ layered domain containing straight pipelines as shown in Fig. 8. The domain consists of three $5 \times 5 \times 10$ layers

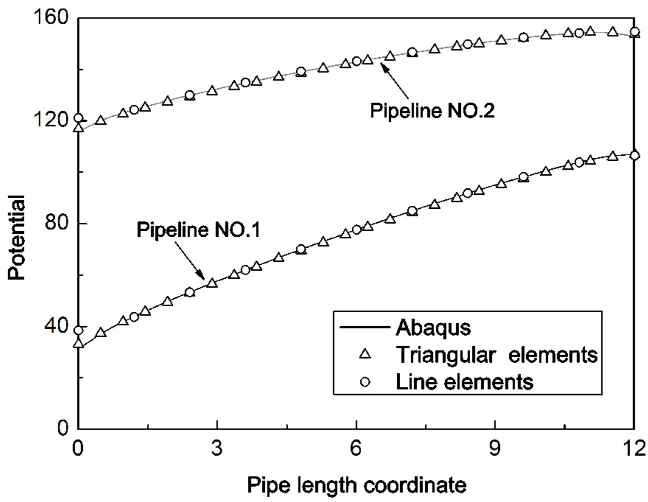

Figure 6: Potentials along the two pipelines in Case No. 2

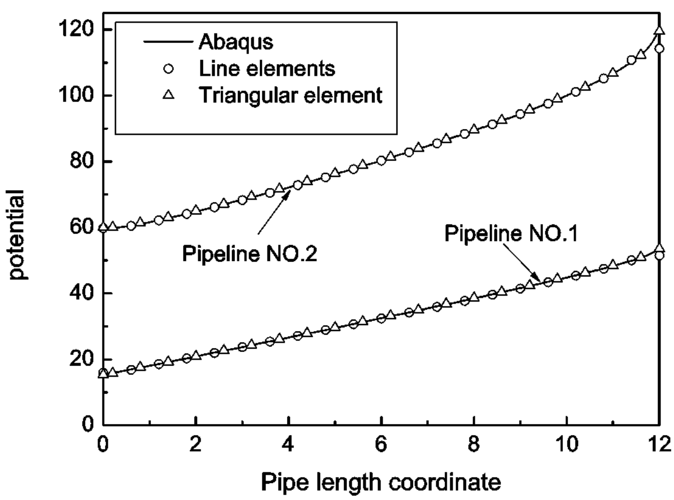

Figure 7: Potentials along the two pipelines in Case No. 3

along the y direction, each containing a pipeline of 8.0 in length along the z direction. The conductivities of the three layers are k = 15.0, 10.0 and 5.0, respectively; the corresponding pipe diameters are 0.2, 0.3 and 0.2, respectively. The bottom and upper ends of each layer are subjected to given potentials as $\bar{\phi} = 70, 40, 10$ and $\bar{\phi} = 150, 120, 90$ respectively, and the rest boundaries are insulated. Two cases of the boundary conditions applied to the pipelines are studied, namely the given potential ($\bar{\phi}_1 = 100$, $\bar{\phi}_2 = 80$, $\bar{\phi}_3 = 60$on the three pipelines respectively) and the nonlinear $\phi - I$ curve (see Fig. 3). In each case, the line model is employed with each pipeline meshed with 16 elements. The total number of unknowns is 10,520. GMRES is adopted as the BEM solver. The numerical results are compared with the FEM.

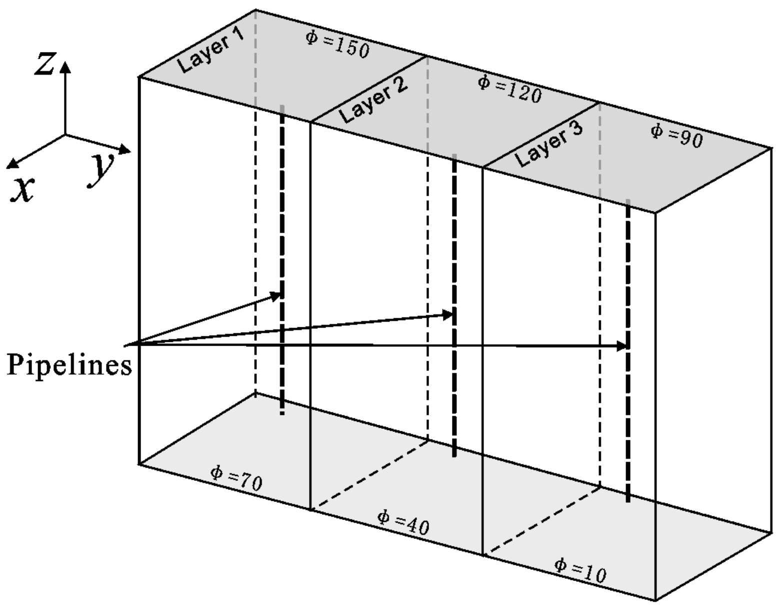

Figure 8: Scheme of a layered domain containing pipelines

Fig. 9 shows a translucent view of the potential distributions in Case No. 1 by using the line model. Figs. 10 and 11 show the results of current densities in Case No. 1 and potentials in Case No. 2 respectively along the pipelines by using the line model and the FEM. Good agreement is observed in both cases. This comparison demonstrates that the presented line model in conjunction with the interface integral BEM is valid for the CP analysis of layered domains containing pipelines with satisfactory accuracy.

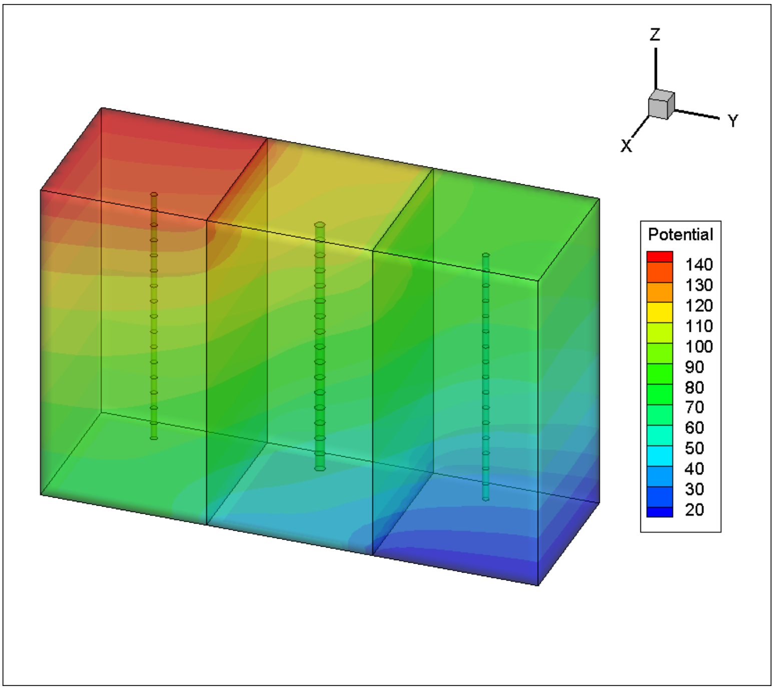

Figure 9: A translucent view of the potential distributions in Case No. 2

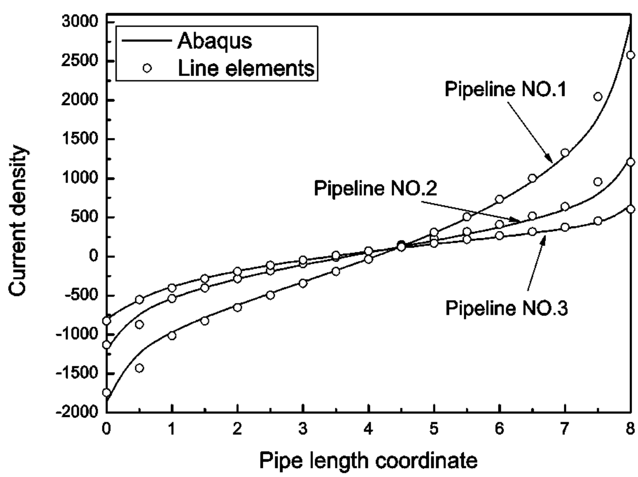

Figure 10: Current densities along the three pipelines in Case No. 1

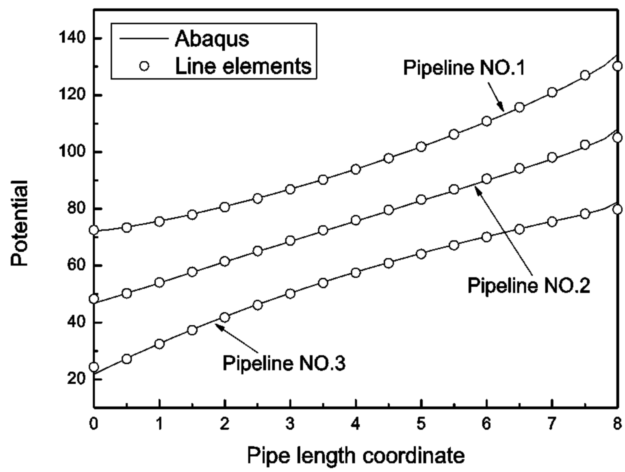

Figure 11: Potentials along the three pipelines in Case No. 2

3.3 Potentials along the large-scale pipelines by using fast multipole BEM

This test involves the CP analysis of a $60 \times 60 \times 60$ homogenous domain containing an array of $5 \times 20 \times 20\,(2000)$ straight pipelines oriented along the z direction. Each pipeline is 10.0 in length and 0.5 in diameter. The conductivity of the domain is taken to be $k = 5.0$. The bottom and upper ends of the domain are subjected to given potentials as $\bar{\phi} = 0$ and 100 respectively, and the rest of its boundaries including the pipelines are insulated. The state of the domain can be treated as an array of 20×20 sub-structures with each containing 5×1 pipelines as shown in Fig. 12. Due to the geometrical symmetry, theoretically potential distributions along the 5×1 pipelines are the same for all sub-structures.

The line model is employed to the domain with each pipeline meshed with 20 elements. The total number of unknowns is 212,800. The fast multipole BEM is adopted as the BEM solver. The calculated potentials along the large-scale pipelines are shown in Fig. 13. The FMM results are compared with a small model solution with only one sub-domain by using GMRES as shown in Fig. 14. Herein the FMM results come from a central sub-structure of the entire domain. Good agreement is observed for all the five pipelines. This comparison demonstrates that the line model-based fast multipole BEM is capable of performing large-scale CP analyses of pipelines with satisfactory accuracy.

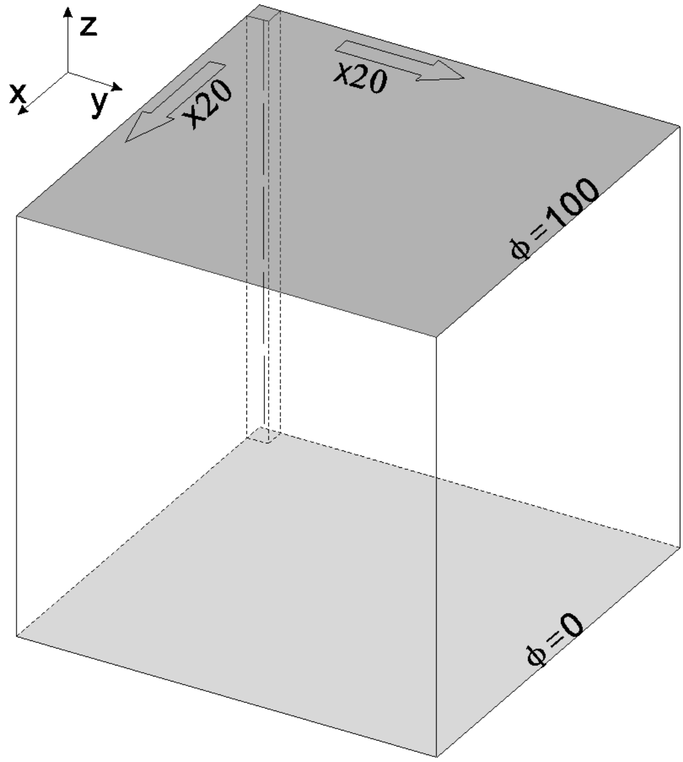

Figure 12: A sub-structure of the domain

3.4 Large-scale analysis of a CP system in the oil industry by using fast multipole BEM

This test involves large-scale analysis of a CP system in the oil industry consisting of an oil tank, layered soils and underground pipelines by using the fast multipole BEM based on the line model. Fig. 15 shows a representative volume of this CP system, where the cylindrical soil domain with 90.0m in diameter is divided into three horizontal layers, each having a thickness of 20.0m; the bottom of an oil tank above the soil is treated as a circular upper boundary of the first soil layer with 40.0m in diameter; three horizontally parallel pipelines, each with 70.0m in length and 1.0m in diameter, are positioned in the central area of the second soil layer with a depth of 30.0m. The gap of the pipelines is 10.0m. The conductivities of the soil layers are 0.05, 0.10 and 0.15 $\Omega^{-1}m^{-1}$, respectively. A sacrificial anode with 20.0m in height and 7.0m in width is positioned at the side of the second soil layer as shown in Fig. 15, and the given potential is $\bar{\phi} = 7.0V$; the bottom of the oil tank

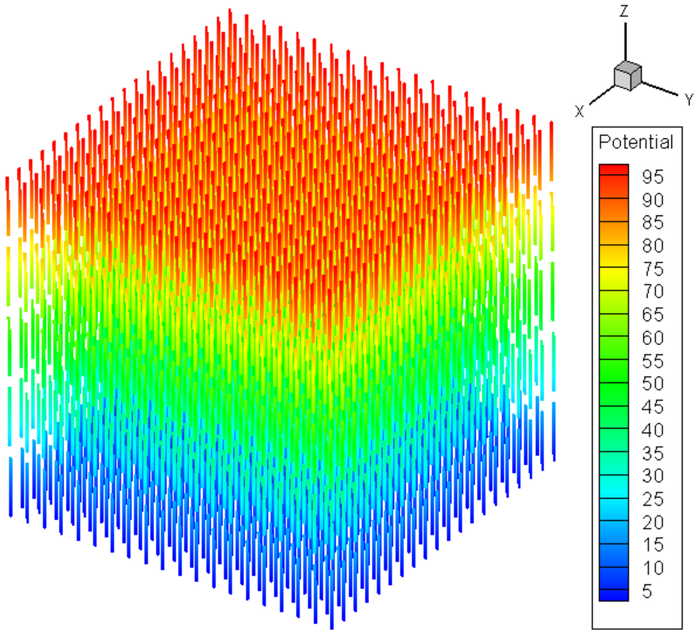

Figure 13: Potential distributions along the large-scale pipelines

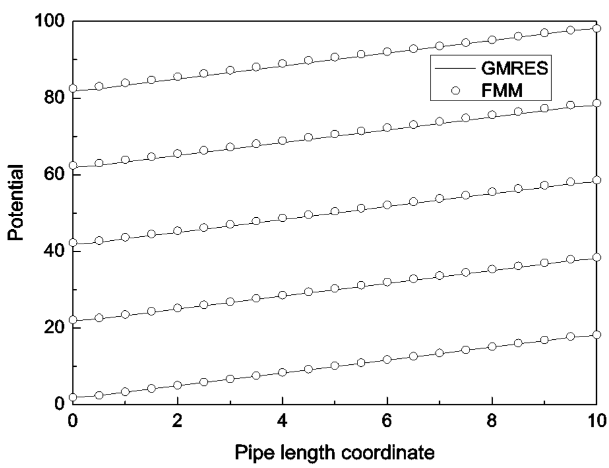

Figure 14: Potentials along the five pipelines in a sub-structure

is given a polarization curve as shown in Fig. 16; the rest boundaries including the pipelines are simply assumed insulated.

The independent boundaries and interfaces of the soil layers are meshed with triangular elements; the pipelines are meshed with line elements. Two mesh densities of the boundary elements are tested for discretizing the model, and the corresponding numbers of unknowns are 8,434 and 41,961, respectively. Fig. 17 shows the boundary elements of the layered soils with fine meshes. GMRES is adopted as the BEM solver for the coarsely meshed model, and the fast multipole BEM is for the finely meshed model. The numerical results are compared with these two solvers. Fig. 18 shows a translucent view of the potential distributions in this CP system with fine meshes. Fig. 19 shows a comparison in the calculated potentials along the central pipeline. It is clearly shown that the results of the fast multipole BEM agree well with the conventional BEM solver, indicating that large-scale CP systems can be solved with satisfactory accuracy by using the fast multipole BEM based on the line model. One can expect that the number of unknowns of the BEM model will be much less than that of the FEM model. Therefore, this technique coupling the boundary-meshing feature of the BEM and the presented method will be competitive with reasonable computer resources in the field of numerical analyses for large-scale CP systems.

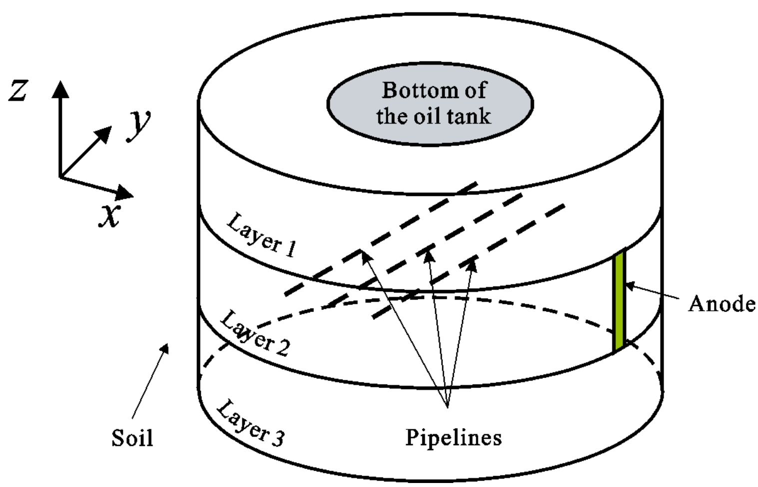

Figure 15: Representative volume of a CP system in the oil industry

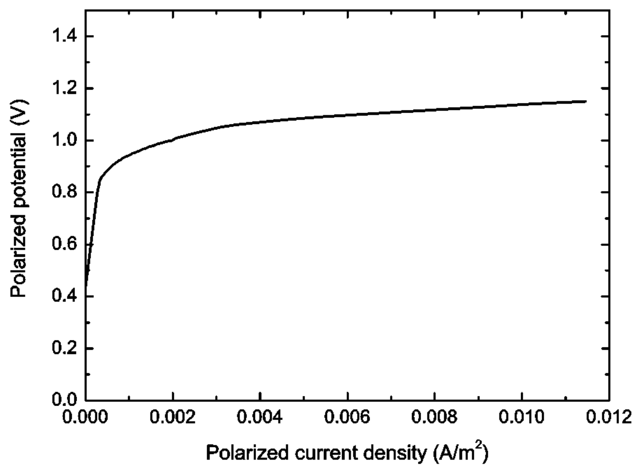

Figure 16: Polarization curve at the bottom of the oil tank

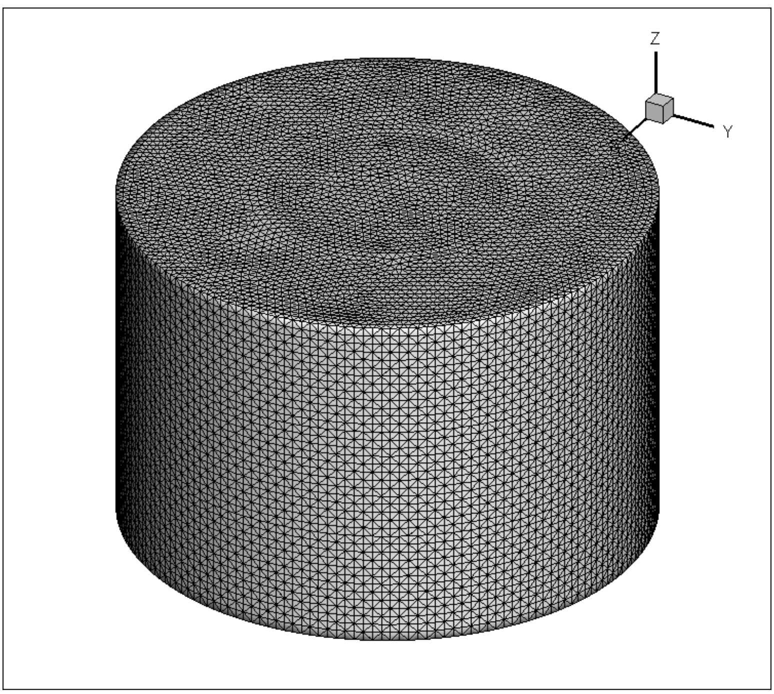

Figure 17: Boundary elements of the layered soils – fine mesh

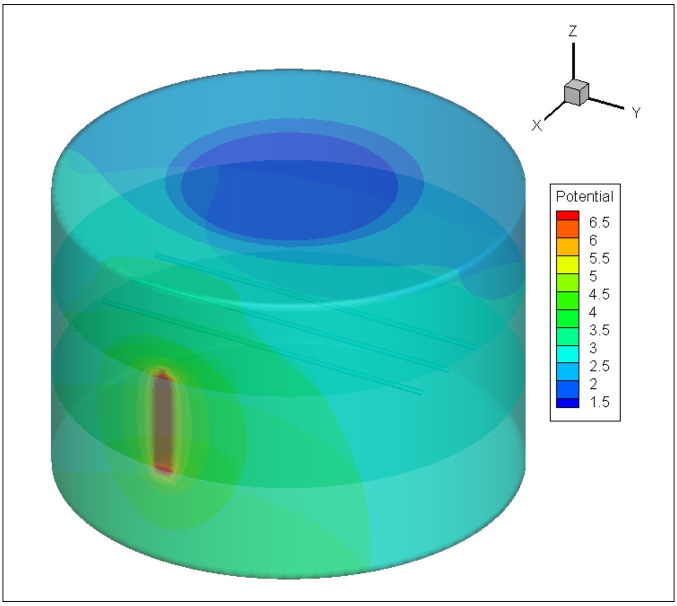

Figure 18: A translucent view of the potential distributions in the CP system

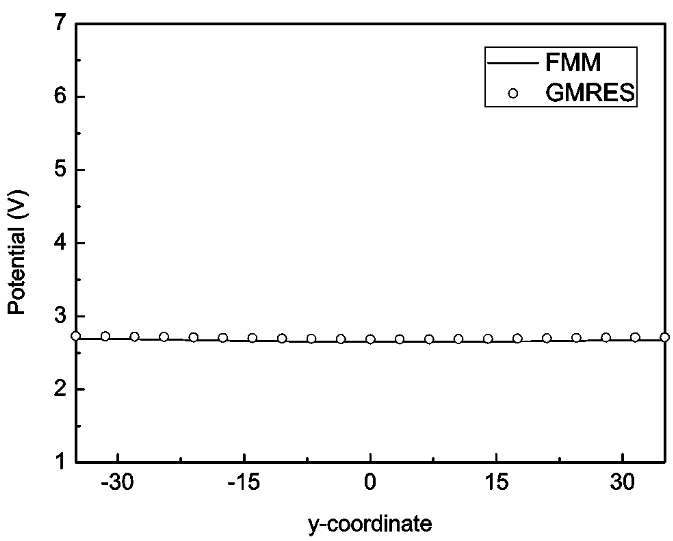

Figure 19: Potentials along the central pipeline

4 Conclusions

A line model-based fast multipole BEM has been developed for the numerical analyses of large-scale CP systems involving pipelines and layered soils in three-dimensions. It is assumed in the line model that current densities and potentials remain constant over any cross-section of the pipelines and vary only along the length direction. Therefore, pipelines can be meshed with line elements and the corresponding required number of unknowns is significantly reduced. The boundary integrals of the line element happen on the original cylindrical surface of the pipeline in order to avoid loss of accuracy due to any shape degeneration. The fast multipole method was employed to accelerate the BEM solutions with a unified formulation of the multipole moments presented for treating mixed types of the boundary elements. An interface integral BEM initially proposed by Gao was applied to govern this multi-domain CP problem with a single-domain formulation.

The proposed line model was firstly applied for the CP analysis of a homogenous domain containing two straight pipelines. The calculated current densities and potentials on the pipelines were found to be in good agreement with that of conventional BEM and FEM. In addition, the required number of unknowns for meshing the pipelines is significantly reduced by using the line model, therefore pipelines with increased scales can be readily analyzed. The model in conjunction with the interface integral BEM was then applied for a multi-domain problem containing pipelines and satisfactory accuracy was observed. Thirdly, the line model-based fast multipole BEM was applied for the CP analysis of large-scale pipelines. The calculated potentials along the pipelines were observed to have good accuracy. Finally, the line model-based fast multipole BEM was applied to analyze a typical CP system in the oil industry involving an oil tank, layered soils and underground pipelines. The results are compared with that of a coarsely meshed model by using the conventional BEM solver and good agreement is observed. In conclusion, the presented method demonstrated its validity in satisfactory accuracy as well as large-scale capability for the CP analyses of pipelines in layered soils.

Acknowledgement

Financial support for the project from the National Natural Science Foundation of China, under grant No. 11072128 is gratefully acknowledged.

References

Adey, R.A.; Niku, S.M. (ASTM STP 1992): Computer modelling of corrosion using the boundary element method. *Comput Model Corrosion*, vol. 1154, pp. 248–264.

Amaya, K.; Aoki, S. (2003): Effective boundary element methods in corrosion analysis. *Engrg Anal Boundary Elements*, vol. 27, pp. 507–519.

Aoki, S.; Amaya, K.; Urago, M.; Nakayama, A. (2004): Fast multipole boundary element analysis of corrosion problems. *CMES: Computer Modeling & Engineering Sciences*, vol. 6, no. 2, pp. 123–131.

Aoki, S.; Arnaya, K.; Imamori, S. (2008): Effective BEM for corrosion analysis of net structure. *Advances in Fracture and Materials Behavior, Pts 1 and 2*, vol. 33-37, no. 1-2, pp. 1299–1302.

Butler, B.M.; Kassab, A.J.; Chopra, M.B.; Chaitanya, V. (2010): Boundary element model of electrochemical dissolution with geometric non-linearities. *Engrg Anal Boundary Elements*, vol. 34, pp. 714–720.

Chen, J.T.; Chen, K.H. (2004): Applications of the dual integral formulation in conjunction with fast multipole method in large-scale problems for 2D exterior acoustics. *Engrg Anal Boundary Elements*, vol. 28, no. 6, pp. 685–709.

Chen, K.H.; Chen, J.T.; Kao, J.H.; Lee, Y.T. (2009): Applications of the dual integral formulation in conjunction with fast multipole method to the oblique incident wave problem. *International Journal for Numerical Methods in Fluids*, vol. 59, no. 7, pp. 711–751.

De Lacerda, L.A.; Da Silva, J.M. (2006): A dual BEM genetic algorithm scheme for the identification of polarization curves of buried slender structures. *CMES: Computer Modeling & Engineering Sciences*, vol. 14, no. 3, pp. 153–160.

Dondero, M.; Cisilino, A.P.; Pablo, T.J. (2011): Numerical Design of Random Micro-Heterogeneous Materials with Functionally-Graded Effective Thermal Conductivities Using Genetic Algorithms and the Fast Boundary Element Method. *CMES: Computer Modeling & Engineering Sciences*, vol. 78, no. 3–4, pp. 225–245.

Druesne, F.; Paumelle, P.; Villon, P. (2000): Application of the BEM to chromium electroplating simulation and toidentification of experimental polarisation laws. *Engrg Anal Boundary Elements*, vol. 24, pp. 615–622.

Gao, X.W.; Wang, J. (2009): Interface integral BEM for solving multi-medium heat conduction problems. *Engrg Anal Boundary Elements*, vol. 33, pp. 539–546.

Greengard, L.; Rokhlin, V. (1997): A fast algorithm for particle simulations. *J Comput Phys*, vol. 135, pp. 280–292.

Greengard, L.; Rokhlin, V. (1997): A new version of the fast multipole method for the Laplace equation in three dimensions. *Acta Numer*, vol. 6, pp. 229–270.

Kyung, J.W.; Tae, S.H.; Lee, H.S. (2007): Potential and current flow of double steel bars in concrete by 2-D BEM. *ISIJ International*, vol. 47, no. 10, pp. 1497–

1503.

Liu, Y.J.; Nishimura, N.; Otani, Y. (2005): Large-scale modeling of carbon-nanotube composites by a fast multipole boundary element method. *Comput Mater Sci*, vol. 34, no. 2, pp. 173–187.

Liu, Y. J.; Nishimura, N.; Otani, Y.; Takahashi, T.; Chen, X. L.; Munakata, H. (2005): A fast boundary element method for the analysis of fiber-reinforced composites based on a rigid-inclusion model. *J Appl Mech*, vol. 72, no. 1, pp. 115–128.

Metwally, I.A.; Al-Mandhari, H.M.; Gastli, A.; Al-Bimani, A. (2008): Stray currents of ESP well casings. *Engrg Anal Boundary Elements*, vol. 32, pp. 32–40.

Miltiadou, P.; Wrobel, L.C. (2002): A BEM-based genetic algorithm for identification of polarization curves in cathodic protection systems. *Int J Numer Methods Engng*, vol. 54, no. 2, pp. 159–174.

Miltiadou, P.; Wrobel, L.C. (2003): Identification of coating defects in cathodically protected underground pipelines. *Int J Numer Methods Engng*, vol. 58, pp. 913–932.

Nishimura, N. (2002): Fast multipole accelerated boundary integral equation methods. *Appl Mech Rev*, vol. 55, no. 4, pp. 299–324.

Ridha, M.; Amaya, K.; Aoki, S. (2005): Boundary element simulation for identification of steel corrosion in concrete using magnetic field measurement. *Corrosion*, vol. 61, no. 8, pp. 784–791.

Rokhlin, V. (1985): Rapid solution of integral equations of classical potential theory. *J Comput Phys*, vol. 60, pp. 187–207.

Wang, H.T.; Yao, Z.H. (2011): A fast multipole dual boundary element method for the three-dimensional crack problems. *CMES: Computer Modeling & Engineering Sciences*, vol. 72, no. 2, pp. 115–147.

Wrobel, L.C.; Miltiadou, P. (2004): Genetic algorithms for inverse cathodic protection problems. *Engrg Anal Boundary Elements*, vol. 28, pp. 267–277.

Yoshida, K. (2001): Applications of fast multipole method to boundary integral equation method. *Ph.D. dissertation, Department of Global Environment Engineering, Kyoto University.*